THE JOURNAL OF BIOLOGICAL CHEMISTRY VOL. 281, NO. 27, pp. 18837–18848, July 7, 2006

Clustering and Coupled Gating Modulate the Activity in KcsA, a Potassium Channel Model*

Received for publication, January 12, 2006, and in revised form, April 27, 2006 Published, JBC Papers in Press, May 2, 2006, DOI 10.1074/jbc.M600342200

Maria L. Molina[‡1], Francisco N. Barrera[‡2], Asia M. Fernández[‡], Jose A. Poveda[‡], Maria L. Renart[‡2], Jose A. Encinar[‡], Gloria Riquelme[§], and Jose M. González-Ros[‡3]

From the [‡]Instituto de Biología Molecular y Celular, Universidad Miguel Hernández, Elche, 03202 Alicante, Spain and the [§]Programa de Fisiología y Biofísica, Instituto de Ciencias Biomédicas, Facultad de Medicina, Universidad de Chile, Casilla 70005, Santiago 7, Chile

Different patterns of channel activity have been detected by patch clamping excised membrane patches from reconstituted giant liposomes containing purified KcsA, a potassium channel from prokaryotes. The more frequent pattern has a characteristic low channel opening probability and exhibits many other features reported for KcsA reconstituted into planar lipid bilayers, including a moderate voltage dependence, blockade by Na^+, and a strict dependence on acidic pH for channel opening. The predominant gating event in this low channel opening probability pattern corresponds to the positive coupling of two KcsA channels. However, other activity patterns have been detected as well, which are characterized by a high channel opening probability (HOP patterns), positive coupling of mostly five concerted channels, and profound changes in other KcsA features, including a different voltage dependence, channel opening at neutral pH, and lack of Na^+ blockade. The above functional diversity occurs correlatively to the heterogeneous supramolecular assembly of KcsA into clusters. Clustering of KcsA depends on protein concentration and occurs both in detergent solution and more markedly in reconstituted membranes, including giant liposomes, where some of the clusters are large enough (up to micrometer size) to be observed by confocal microscopy. As in the allosteric conformational spread responses observed in receptor clustering (Bray, D. and Duke, T. (2004) *Annu. Rev. Biophys. Biomol. Struct.* 33, 53–73) our tenet is that physical clustering of KcsA channels is behind the observed multiple coupled gating and diverse functional responses.

During the last decades, the use of high resolution electrophysiological techniques to study ion channels has provided a large amount of information on functional aspects of these important membrane proteins. Such a detailed information on channel function, however, has not been accompanied by structural knowledge until recently, when several structurally simpler homologues of mammalian ion channels found in extremophyle bacteria or *Archaea* and remarkably resistant to harsh experimental conditions, have been purified, crystallized and their structure solved at high resolution by x-ray diffraction methods (1–4). A K^+ channel from the soil bacteria *Streptomyces lividans* named KcsA[4] (1), a homotetramer made up of identical 160-amino acid subunits, was the first of such structures to be solved (5, 6), and, although the x-ray structure corresponds to a closed channel conformation, it has contributed much to our current understanding of ion selectivity and permeation. Ironically, there was little or no functional information on KcsA by the time its structure was solved, and then several groups undertook the task of characterizing its single channel properties, which has been surrounded by controversy. For instance, Schrempf's group, discoverers of KcsA in *S. lividans*, reported a strong dependence of channel opening on acidic pH, multiple conductance states with opening probabilities near 0.5, and unusual permeabilities to Na^+, Li^+, Ca^{2+}, or Mg^{2+}, along with K^+ (7–9). In contrast, Miller's group (10, 11) using purified KcsA reconstituted into planar lipid bilayers found a single conductance state with a much lower opening probability, as well as orthodox ion selectivity and other properties to validate KcsA as a *bona fide* K^+ channel and as a faithful structural model for these molecules. The above discrepancies were never fully explained but, still, it became generally accepted that KcsA behaves as a moderately voltage-dependent, K^+-selective channel with a characteristic low opening probability and the peculiar property of opening only in response to very acidic pH conditions at the intracellular side of the membrane. More recently, however, it was found that KcsA opens also at neutral pH when subjected to an outward K^+ gradient (12). Furthermore, it has been proposed that a more "physiological" version of KcsA might correspond to a supramolecular conductive complex in which the channel would coassemble with polyhydroxybutyrate and inorganic polyphosphates (13), which are abundant reservoir materials in many prokaryotes.

In this report we have used excised membrane patches from reconstituted giant liposomes containing purified KcsA. Through the analysis of a large number of patch clamp recordings we found a clearly diverse functional behavior for the KcsA channel. The more frequent pattern of activity corresponds to the low opening probability and acidic pH-dependent channel referred above, but other activity patterns have been detected as well, which are characterized by a high channel opening probability at both acidic and neutral pH. As an additional salient feature, the latter recordings show frequent coupled gating involving multiple channels. These observations are unprecedented, and we interpret them based on the additional finding that heterogeneous "cluster"-like supramolecular assemblies of KcsA are formed, into which the channels adopt different, integrated behaviors.

* This work was supported in part by the Spanish Dirección General de Investigación (Grant BFU2005-00749), the Agencia Valenciana de Ciencia y Tecnología (Grant 03/056), and the Chilean FONDECYT (Grant 1040546). The costs of publication of this article were defrayed in part by the payment of page charges. This article must therefore be hereby marked "*advertisement*" in accordance with 18 U.S.C. Section 1734 solely to indicate this fact.

[1] Had a predoctoral fellowship from the Generalitat Valenciana.

[2] Supported by predoctoral fellowships from the Ministerio de Educación y Ciencia of Spain.

[3] To whom correspondence should be addressed: Instituto de Biología Molecular y Celular, Universidad Miguel Hernández, Elche, 03202 Alicante, Spain. Tel.: 34-96-665-8757; Fax: 34-96-665-8758; E-mail: gonzalez.ros@umh.es.

[4] The abbreviations used are: KcsA, potassium channel from *S. lividans*; DDM, dodecyl β-D-maltoside; LOP pattern, low channel opening probability pattern of KcsA; HOP pattern, high channel opening probability pattern of KcsA; FRET, fluorescence resonance energy transfer; Alexa 546, Alexa fluor® 546 C5 maleimide; Alexa 647, Alexa fluor® 647 C2 maleimide; NBD-DMPE, *N*-(7-nitrobenz-2-oxa-1,3-diazol-4-yl)-1,2-dihexadecanoyl-*sn*-glycero-3-phosphoethanolamine; PBS, phosphate-buffered saline.

EXPERIMENTAL PROCEDURES

Constructs and Mutants—The wild-type KcsA construct contained the *kcsA* gene of *S. lividans* cloned in-frame into the pQE30 vector (Qiagen), which provided ampicillin resistance and a N-terminal hexahistidine tag (14). The KcsA S22C mutant was obtained (QuikChange site-directed mutagenesis kit, Stratagene) by generating PCR fragments using pairs of complementary mutant primers, sense primer 5′-CTC GGG CGC CAC GGC TGT GCG CTG CAC TGG and antisense primer 5′-CCA GTG CAG CGC ACA GCC GTG GCG CCC GAG. The KcsA S22C mutant sequence was verified by dideoxy-nucleotide sequencing.

Protein Expression and Purification—Expression of the wild-type KcsA protein and the KcsA S22C mutant in *Escherichia coli* M15 (pRep4) cells, and its purification by affinity chromatography on a nickel-nitrilotriacetic acid-agarose column, was carried out as reported previously (14). The purified protein consisted primarily of the characteristic SDS-resistant tetramer, which is accompanied by monomeric KcsA as a minor component and in sufficiently loaded SDS-PAGE gels, by higher molecular weight, SDS-resistant KcsA multimers. All the above KcsA species were immunoreactive against commercial anti-His tag monoclonal antibodies (see the *inset* to Fig. 8*A*).

The expression yields and the SDS-PAGE profile of the KcsA S22C mutant were very similar to those exhibited by the wild-type KcsA. The protein concentration was determined by the DC-Protein colorimetric assay (Bio-Rad), relative to a bovine serum albumin standard. When expressed in molar terms, the protein concentration refers to KcsA tetramers. 1–125 KcsA was prepared by chymotrypsin hydrolysis of wild-type KcsA as described earlier (14).

Reconstitution of Proteins into Asolectin Lipid Vesicles and Preparation of Giant Liposomes—Batches of large unilamellar vesicles of asolectin (soybean lipids, type II-S, Sigma) were prepared at 25 mg/ml as described earlier (15) in 10 mM Hepes, pH 7.0, 100 mM KCl (reconstitution buffer) and stored in liquid N_2. The purified DDM-solubilized protein (wild-type KcsA, 1–125 KcsA, or fluorescently labeled KcsA S22C derivatives, depending on the different experiments) was mixed with the above asolectin vesicles previously resolubilized in 3 mM DDM. Reconstituted liposomes were formed by removing the detergent by gel filtration (14). The protein-containing reconstituted vesicles eluted in the void volume and were pooled, centrifuged 30 min at 300,000 × *g*, resuspended at 1 mg of protein/ml in reconstitution buffer, divided into aliquots, and stored in liquid N_2.

Multilamellar giant liposomes (up to 50–100 μM in diameter) were prepared by submitting a mixture of the reconstituted vesicles (usually containing 50 μg of protein) and asolectin lipid vesicles (25 mg of total lipids) to a cycle of partial dehydration/rehydration (15), with the exception that the dehydration solution used here was 10 mM Hepes (potassium salt) buffer, pH 7, containing 5% ethylene glycol and the rehydration solution was 10 mM Hepes (potassium salt) buffer, pH 7. As a control, each of the different batches of asolectin vesicles was also used to prepare protein-free giant liposomes. Those liposome batches, posing difficulties to obtain high resistance seals (see below) or showing erratic baselines in the patch clamp recordings because of remaining detergent or other reasons, were discarded.

Electrophysiological Recordings—For patch clamp measurements of channel activity, aliquots (3–6 μl) of giant liposomes were deposited onto 3.5-cm Petri dishes and mixed with 2 ml of the buffer of choice for electrical recording (bath solution; usually 10 mM Mes buffer, pH 4, containing 100 mM KCl). Giga seals were formed on giant liposomes with borosilicate microelectrodes (Sutter Instruments) of 7–10 megohms open resistances, filled with 10 mM Hepes buffer, pH 7, 100 mM KCl (pipette solution). After sealing, excised inside-out patches were obtained by withdrawing the pipette from the liposome surface. Standard patch clamp recordings (16) were obtained using either Axopatch 200A (Axon Instruments, Union City, CA) or EPC-9 (Heka Electronic, Lambrecht/Pfalzt, Germany) patch clamp amplifiers, at a gain of 50 mV/pA. The holding potential was applied to the interior of the patch pipette, and the bath was maintained at virtual ground ($V = V_{bath} - V_{pipette}$). An Ag-AgCl wire was used as the reference electrode through an agar bridge, and the junction potential was compensated when necessary. Routinely, the membrane patches were subjected to a protocol of pulses and/or voltage ramps. The protocol of pulses went from −200 to +200 mV, at 50-mV intervals, and 2 s of recording at each individual voltage was used, holding the patch back to 0 mV between the different voltage steps. The voltage ramps went from −200 to +200 mV, during a 3-s scan. All measurements were made at room temperature. Recordings were filtered at 1 kHz, and the data were analyzed off-line with the pClamp9 software (Axon Instruments).

Recordings from giant liposomes prepared from either 50 or 100 μg of wild-type KcsA protein and registered under identical experimental conditions (pH 4 at the bath and pH 7 at the pipette solutions) exhibited qualitatively similar patterns of ion channel activity but differed in complexity (a larger number of events as the amount of protein increased) and in the percent of silent patches, which went from only 9% ($n = 23$) when using 100 μg of protein, to ~38% ($n = 150$) for 50 μg of protein, respectively. Thus, for practical purposes, we studied in more detail the giant liposomes made from 50 μg of protein, which became our "standard" experimental condition.

SDS-PAGE and Western Immunoblotting—For SDS-PAGE analysis, the protein-containing samples were mixed with an equal volume of electrophoresis buffer sample (20 mM Tris, pH 6.8, 20% glycerol, 0.1% bromphenol blue, and 4% SDS) and applied to a 13.5% acrylamide gel in the presence of 0.1% SDS (17). After electrophoresis, proteins were transferred onto a nitrocellulose membrane. Blots were incubated with 3% (w/v) bovine serum albumin in PBS-T (phosphate-buffered saline, pH 7.4, containing 0.05% Tween 20). The His-tagged KcsA was detected with a mouse monoclonal anti-Tetra-His antibody (1:1000 dilution, Qiagen) in PBS-T. After washing, the immunoblots were incubated with a secondary horseradish peroxidase-conjugated rabbit anti-mouse IgG (1:1000, Sigma) in PBS-T. Immunoreactive proteins were visualized by chemiluminescent ECL detection reagent (Amersham Biosciences).

Analytical Ultracentrifugation—Sedimentation velocity experiments were conducted in a Beckman Optima XL-I ultracentrifuge (Beckman Coulter) with an An50Ti eight-hole rotor and double-sector Epon-charcoal centerpieces. DDM-solubilized KcsA samples at protein concentrations ranging 0.5–10 μM in 20 mM Hepes buffer, pH 7.0, containing 100 mM KCl and 5 mM DDM, were centrifuged at 40,000 rpm, 20 °C, and the absorbance at 280 nm was followed. Differential sedimentation coefficient distributions, $c(s)$, were calculated by least-squares boundary modeling of sedimentation velocity data by using the program SEDFIT (18, 19).

Fluorescence Labeling of KcsA—Aliquots of the sulfhydryl-containing mutant KcsA S22C at 7 μM in 20 mM Hepes, pH 7, 100 mM KCl and 5 mM DDM were treated for 1 h in the dark with a 10-fold molar excess of Tris(2-carboxyethyl)phosphine hydrochloride to keep the sulfhydryl groups in a reduced form. The maleimide Alexa probes (Alexa Fluor® 546 C5-maleimide or Alexa Fluor® 647 C2-maleimide; Molecular Probes) were dissolved in buffer and added in a

10-fold molar excess to the reduced KcsA samples. After 2-h incubation at 4 °C, an excess of 2-mercaptoethanol was added to react with the excess free probe. Finally, the fluorescently labeled KcsA was separated from the free fluorophores by gel filtration on Sephadex G-50 (medium), which also eliminates the minor population of monomeric KcsA present in the purified KcsA preparations. Monitoring of the absorbance at either 546 or 647 nm was used to define the elution profile, while the protein was detected by SDS-PAGE of the different fractions. Routinely, yields ranging 20 to 30% labeling of the available sulfhydryls were obtained.

Fluorescence Anisotropy Measurements—Stock solutions of Alexa 546-labeled KcsA in 10 mM Hepes buffer, pH 7.0, 100 mM KCl, and 5 mM DDM were subjected to successive dilutions with the same buffer to attain different protein concentrations. Steady-state fluorescence anisotropy $\langle r \rangle$ was determined at 25 °C in an SLM-8000C spectrofluorometer equipped with Glan-Thompson polarizers in the "L" format, by measuring the vertical (I_{VV}) and horizontal (I_{VH}) components of the fluorescence emission with excitation polarized vertically, as defined by (20),

$$\langle r \rangle = (I_{VV} - G^*I_{VH})/(I_{VV} + 2^*G^*I_{VH}) \quad \text{(Eq. 1)}$$

where the G factor ($G = I_{HV}/I_{HH}$) corrects for the transmission bias introduced by the detection system. Excitation and emission wavelengths were 525 and 574 nm, respectively. The protein and DDM concentration were low enough to prevent scattering artifacts that could result in an artificial depolarization of the fluorescence. Similar measurements carried out using Alexa 647-labeled KcsA yielded essentially identical results.

Fluorescence Resonance Energy Transfer Measurements—Alexa 546- and Alexa 647-labeled KcsA were used as the donor-acceptor pair for FRET measurements both in detergent solution (10 mM Hepes buffer, pH 7, 100 mM KCl, 5 mM DDM) and in reconstituted asolectin lipid vesicles. For the latter, the reconstituted vesicles were prepared at a fixed asolectin lipid to total protein weight ratio of 10:1 in 10 mM Hepes buffer, pH 7, 100 mM KCl. Because the donor concentration (~6 μg of protein/ml) was not identical in the different samples, particularly in the reconstituted vesicles, FRET efficiency (E) was not calculated through the usual method of quenching of donor steady-state emission. Instead, two other approaches were used. In the first approach, E was determined by measuring the increase in fluorescence of the acceptor due to energy transfer and comparing this to the residual donor emission (21). For this, steady-state emission scans of the samples at different donor to acceptor ratios were recorded in an SLM-8000C spectrofluorometer at an excitation wavelength of 525 nm and at emission wavelengths from 540 to 750 nm at 1-nm intervals, and corrected for background and instrument response. The acceptor emission coming from its direct excitation at 525 nm was negligible in the reconstituted samples but not in detergent solution, where such contribution was always subtracted. Afterward, the spectra were normalized to the donor maximum at 574 nm where there is no acceptor fluorescence. Then, the donor spectrum was subtracted from each of the donors plus acceptor spectra, and the integrated areas of the resulting curves were calculated (I_{AD}). The area under the donor spectrum was also calculated (I_D), and then E results from,

$$E = (I_{AD}/q_A)/(I_D/q_D + I_{AD}/q_A) \quad \text{(Eq. 2)}$$

where q_A (0.80) and q_D (0.85 (22)) are the experimentally determined quantum yields of the acceptor and donor, respectively.

The second approach estimates the transfer efficiency in samples with different donor concentration from measurements of the donor fluorescence decay at different donor to acceptor ratios. Fluorescence decays were measured in a fluorescence lifetime instrument (Photon Technology International Inc.) using a proprietary stroboscopic detection technique (23, 24). The system used a GL-330 pulsed nitrogen laser pumping a GL-302 high resolution dye laser. The dye laser output at 525 nm was fitted to the sample compartment via fiber optics. The emission wavelength was 574 nm. Fluorescence decays were analyzed using a non-linear least-squares regression method. The average decay times, which are proportional to the steady-state intensities, were calculated from the results of multiexponential fits by using the expression,

$$\langle \tau \rangle = (\Sigma a_i \tau_i)/(\Sigma a_i) \quad \text{(Eq. 3)}$$

where a_i and τ_i represent the pre-exponential factors and the lifetimes, respectively. From these, E was calculated using the expression (20),

$$E = 1 - \tau_{DA}/\tau_D \quad \text{(Eq. 4)}$$

where τ_{DA} and τ_D are the average fluorescence lifetimes of the donor in the presence and in the absence of acceptor, respectively.

Finally, the theoretical contribution to FRET arising purely from the random distribution of labeled KcsA donors and acceptors within the two-dimensional membrane bilayer was estimated according to Capeta *et al.* (25). Such calculations take into account three parameters, β_w, β_1, and B. β_w, the interplanar spacing between donors and acceptors, was fixed to zero, because both probes are located at cysteine 22 in different KcsA molecules. β_1 is the ratio R_1/R_0, where R_1, the exclusion distance, represents the minimal distance between two probes, and R_0 is the Förster's distance. R_1 was fixed as twice the protein radius (51.9 Å in the KcsA crystal structure), whereas R_0 was 68 Å as calculated from the spectral overlap and the donor quantum yield. B, the relative enrichment factor for the acceptor in the proximities of the donor was fixed to 1.05, which assumes a random distribution of donors and acceptors in the bilayer. A similar theoretical curve was also obtained by applying other models such as that from Wolber and Hudson (26).

Confocal Fluorescence Microscopy—Aliquots (3–6 μl) of giant liposomes containing fluorescently labeled KcsA were deposited on a coverslip mounted on a custom-made chamber and mixed with 1 ml of 10 mM Hepes buffer, pH 7.0, 100 mM KCl. The samples were visualized without any further treatment by using an LSM 5 Pascal confocal laser scanning microscope (Axiovert 200M, Carl Zeiss) and a Plan-Neofluar 40×/1.3 objective. Giant liposomes containing Alexa 546-labeled KcsA were excited with the 543 nm line of an argon laser, and the emitted light was filtered through a 560–615 nm band pass filter. For giant liposomes containing Alexa 647-labeled KcsA, the 633 nm line of a He-Ne laser was used for excitation, whereas the emitted light was filtered through a 650 nm long pass filter. For FRET images, giant liposomes containing both Alexa 546- and Alexa 647-labeled KcsA, usually at a 1:1 donor/acceptor ratio, were excited at the above 543 nm emission line of the argon laser and the emission was filtered through the 650 long pass filter. These conditions do not require any spectral bleed-through correction.

Giant liposomes containing the fluorescently labeled phospholipid NBD-DMPE, added (0.05%) to the asolectin lipids during reconstitution, were visualized by exciting the NBD-DMPE probe with the 488 nm emission line of the argon laser and using a 505–560 nm band pass emission filter.

RESULTS

Diverse Functional Behavior of KcsA: Low and High Channel Opening Probability Patterns—Unless stated otherwise, excised membrane patches from giant liposomes prepared from 50 μg of purified KcsA and 25 mg of asolectin lipids (see "Experimental Procedures") were always used in these experiments. The recording bath solution was 10 mM Mes buffer, pH 4, containing 100 mM KCl, whereas the pipette solution was 10 mM Hepes buffer, pH 7, 100 mM KCl. Despite the identical experimental conditions, different types of activity were distinguished in these patches ($n = 93$) and classified as "low" or "high" channel opening probability patterns based on the probability of finding channel opening events in the recordings (Fig. 1). These experiments used a large number of different batches of both purified KcsA and asolectin lipids to prepare the giant liposomes. However, we found no dependence with either the moment in which the experiments were carried out or with the different batches used. Moreover, the different activity patterns illustrated in Fig. 1 were often observed in different patches from the same preparation of giant liposomes.

Fig. 1 shows typical voltage ramps from protein-free patches used as a control (Fig. 1*A*), as well as from different KcsA-containing patches representative of the different opening probability patterns observed. Fig. 1*B* shows a few openings in the form of bursts of activity, but the channels are closed most of the time, which are well known reported features of KcsA (10, 11). Accordingly, we named this pattern "low channel opening probability" or LOP pattern, seen in 55% of the recordings ($n = 51$). On the contrary, Fig. 1 (*C* and *D*) shows examples of activity patterns in which the most salient feature is that the channels are opened most of the time. These patches were named as "high channel opening probability" or HOP patterns and were observed in 45% of the cases ($n = 42$), including some instances in which somewhat intermediate behaviors between those depicted in Fig. 1 (*C* and *D*) were detected in the recordings. The predominant HOP pattern corresponds to that in Fig. 1*C* ($n = 26$), in which similar current is conducted at either positive or negative potentials, following an almost symmetrical sigmoid-like voltage dependence. Characteristically, channel closings are observed at extreme voltages and variable flickering may sometimes be present at any of the voltages studied. Fig. 1*D* shows a different HOP pattern encountered with a lower incidence ($n = 10$) in which more current is conducted at negative than at positive voltages, thus showing an inward rectifier behavior. These latter recordings do not show a predominance of channel closings at the extreme values in the voltage ramps, while variable flickering (from moderate to very intense) may also be present. This variability observed when KcsA is reconstituted into giant liposomes was not explicitly reported in the earlier characterization of KcsA in planar lipid bilayers, but it seems reminiscent of that referred more recently (27) using the latter reconstituted system.

Regardless of the pattern exhibited, additional experiments carried out under asymmetrical KCl concentrations (400 and 100 mM KCl in the bath and pipette solutions, respectively, under otherwise identical conditions) yielded very similar reversal potentials, which were near that corresponding to potassium under these gradient conditions (not shown).

Curiously, a small population of patches ($n = 6$) was also found in which the main feature was that the number of open channels increased progressively in a "ladder"-like manner during the time course of the recordings as the protocol of pulses was applied repetitively. This latter behavior is discussed below under "Results."

Analysis of the LOP Pattern—In agreement with previous reports, channel opening in this activity pattern requires acidic pH (8–11, 28). Fig. 2*A* shows that these excised membrane patches do not exhibit

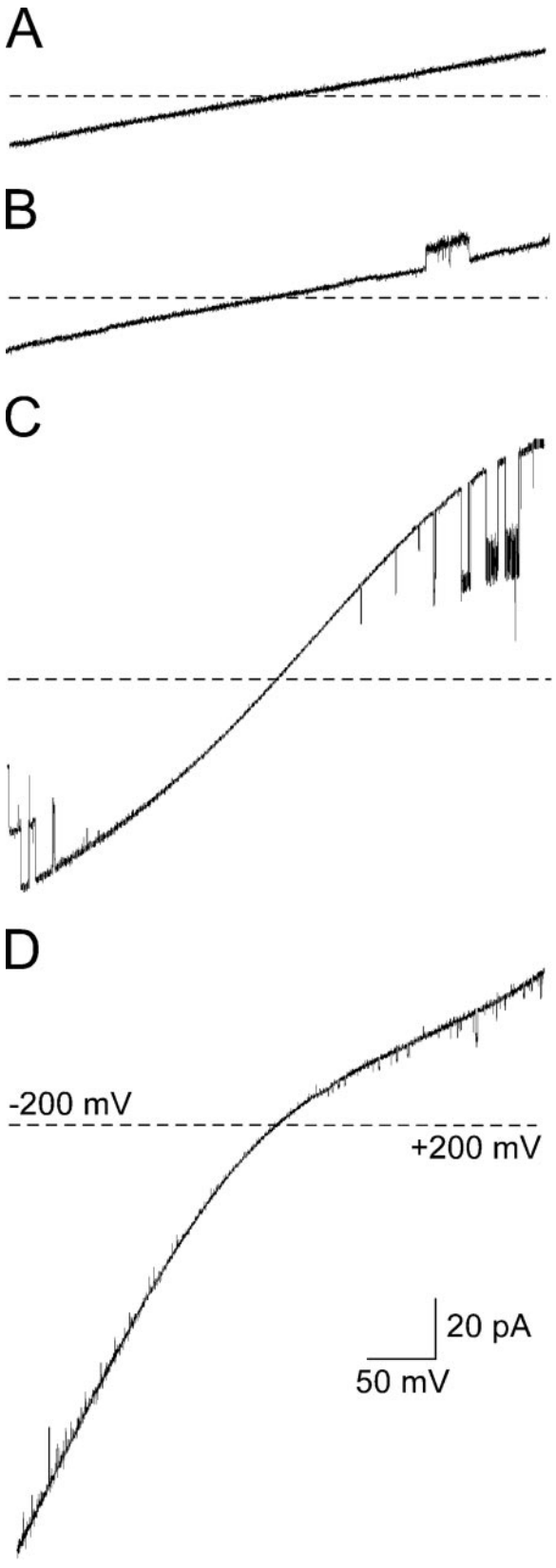

FIGURE 1. **Diverse functional behavior of KcsA.** Typical voltage ramps obtained under identical experimental conditions by patch clamping excised inside-out patches from reconstituted giant liposomes prepared in the absence (*A*) or in the presence of the purified KcsA channel. *B*, slightly predominant low channel opening probability (LOP) pattern; *C* and *D*, high channel opening probability (HOP) patterns exhibiting either symmetrical sigmoid-like voltage dependence (*C*) or inward rectifier-like behavior (*D*).

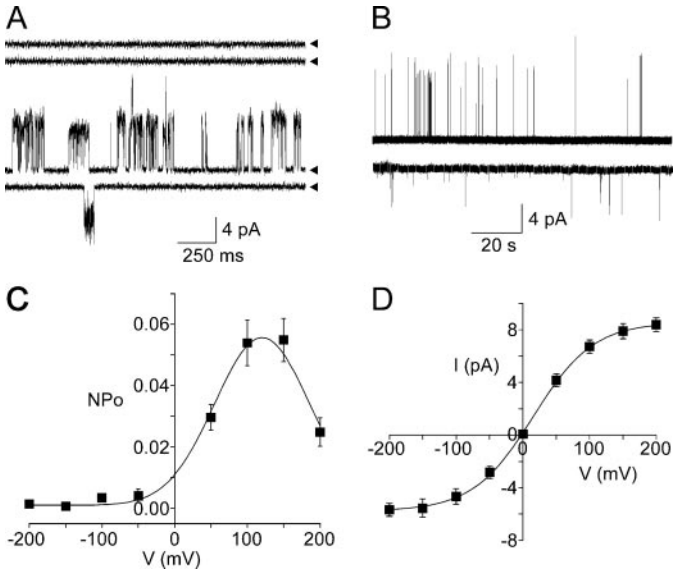

FIGURE 2. **Main features of the LOP pattern of KcsA.** *A*, acidic pH dependence of channel opening. The *upper traces* illustrate the lack of channel activity when 100 mM KCl symmetrical solutions at pH 7 were used at both sides of the patch at ±150 mV. The *bottom traces* were obtained by changing the bath solution to pH 4. In this and all similar figures, closed channel states are indicated by *arrowheads*. *B*, representative long recordings of channel activity at ±150 mV to illustrate the characteristic rapid gating in the form of bursts of activity within long-lived silent periods. Unless indicated otherwise, the pH values of the bath and pipette solutions in this and all following figures were 4 and 7, respectively (see "Experimental Procedures"). *C*, voltage dependence of the channel opening probability (NP_o) calculated as the fraction of time during which the channels are opened in recordings ranging from 30 s to 2 min in length ($n = 6$). *D*, open channel current *versus* voltage curve, obtained by averaging the current amplitudes from several different patches ($n = 9$). The results shown in *C* and *D* and in all other similar figures are the mean ± S.E.

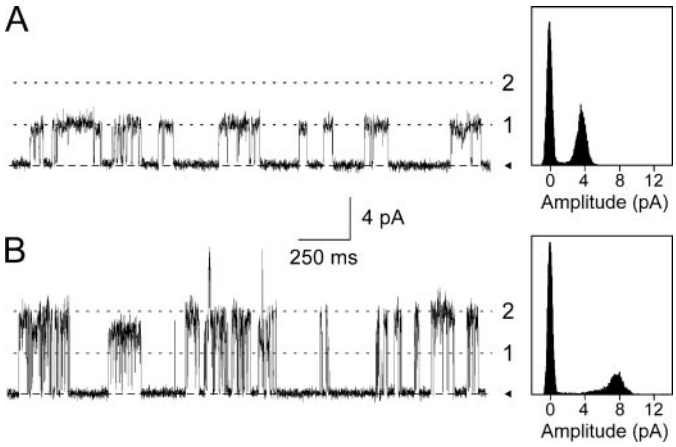

FIGURE 3. **Coupled gating of KcsA channels in the LOP pattern.** *A*, a recording containing only the minimal 4-pA single channel currents seen at +150 mV; *B*, a recording obtained under identical conditions but containing predominant 8-pA currents resulting from coupling of two KcsA channels. The amplitude histograms of each of the above recordings are shown to the *right*. The latter 8-pA currents were the predominant events in most recordings of KcsA taken in LOP patterns. The *dashed lines* in the two recordings (labeled '*1*' and '*2*') are indicative of the 4- and 8-pA current levels.

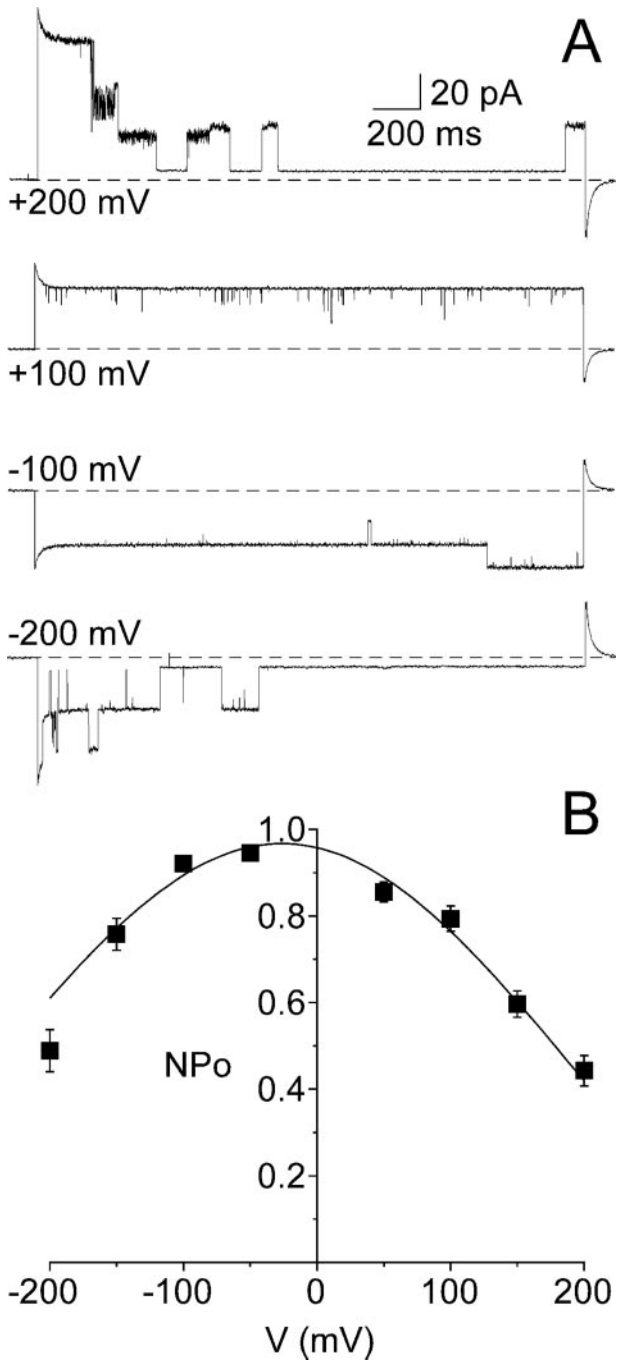

FIGURE 4. **Main features of a HOP pattern of KcsA, such as that shown in Fig. 1C.** *A*, shows representative channel currents taken at ±100 mV, where the channels are opened during most of the recording, or at ±200 mV in which channel closings are more likely to occur. Due to the difficulties in identifying the closed state in some of these recordings, the *dashed lines* indicate the zero current levels. *B*, shows the voltage dependence of the open channel probability (NP_o) calculated as the fraction of time during which the channels are opened in recordings such as those shown in *A* ($n = 6$), which exceeded 0.9 near 0 mV and decreased at the extreme voltages used in these studies.

channel opening events when symmetrical solutions at pH 7 were maintained in the bath and pipette sides of the patch. On the contrary, changing the bath solution to pH 4 causes channel opening activity (Fig. 2*A*, *lower traces*), regardless of whether the pipette solution was maintained at pH 4 or 7. These pH-dependent changes in gating behavior are produced immediately upon perfusion of the bath solution and are also fully reversible. Finally, changing the pipette solution to pH 4, while leaving the bath solution at pH 7, results in only occasional channel openings (not shown). All the above indicates that the acidic pH-sensing sites in our excised patches are mostly exposed to the bath solution. Using point mutations in the KcsA structure, it was elegantly demonstrated that the characteristic pH sensitivity of this channel was confined to its intracellular portion (10), thus, it should be concluded that our excised patches are "inside-out," with the cytoplasmic portion of KcsA oriented toward the bath side.

Fig. 2*B* shows representative recordings of channel activity at two different holding potentials. The recordings typically show rapid gating

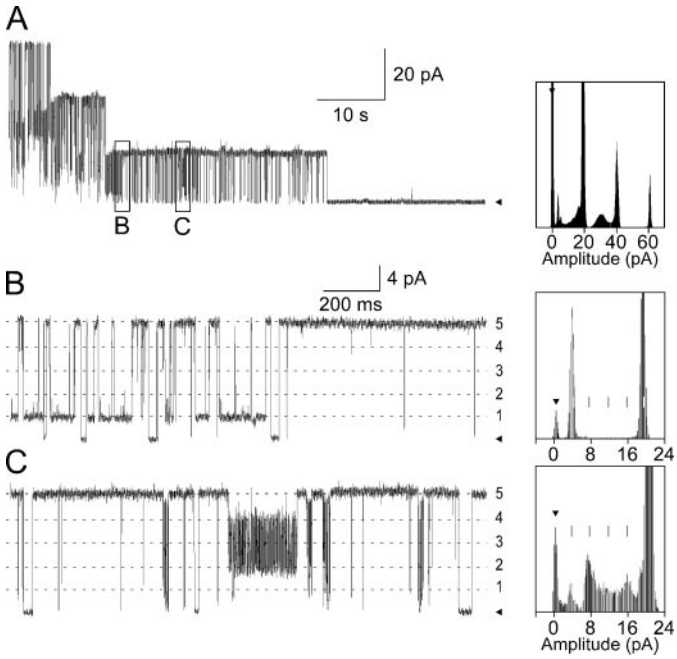

FIGURE 5. **Coupled gating of KcsA channels in HOP patterns.** *A*, a representative recording taken at +150 mV illustrating three successive closings of 20-pA current levels in a HOP pattern similar to that shown in Fig. 1*C*. *B* and *C*, some regions of the above recording in more detail, in which, in addition to the main 20-pA current level, openings and closings of a smaller 4-pA current could also be observed, along with other currents whose intensities are integer multiples of the smaller 4-pA currents. The main gating event, however, corresponds to the 20-pA currents, which seemingly result from the positive coupling of five of the smaller 4-pA current levels. The amplitude histograms of each of the above recordings are shown to the *right*. *Dashed lines* in *B* and *C* (flanked by numbers '*1*' through '*5*') are solely to indicate the 4-, 8-, 12-, 16-, and 20-pA current levels.

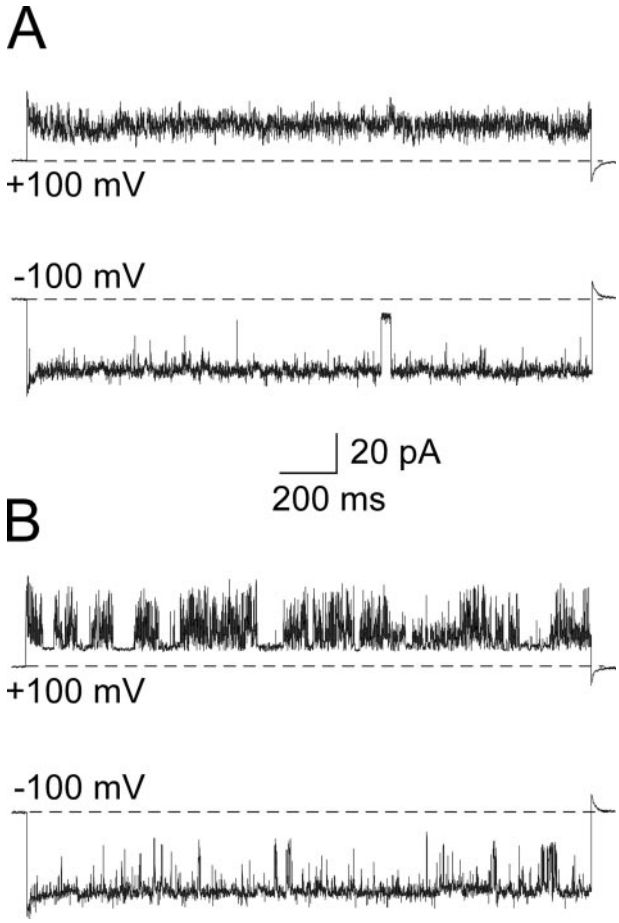

FIGURE 6. **Channel opening of KcsA in HOP patterns does not depend on acidic pH.** *A*, shows recordings of channel activity taken at ±100 mV using the usual solutions at pH 4 in the bath and pH 7 in the pipette. *B*, shows recordings taken under identical conditions except that the pH in the bath solution was also 7. The *dashed lines* indicate the zero current levels.

in bursts of activity within long-lived silent periods. Channel openings are somewhat variable in amplitude, particularly at positive voltages, and quite noisy, mostly at negative voltages. These recordings were used to calculate the open channel probability (Fig. 2*C*), as the fraction of time during which the channels are opened. Such values were lower than 0.06 ($n = 6$), which is in fair accordance with reports by others (29) and exhibited a bell-shaped voltage dependence with a maximum at ~+120 mV. The regions of these recordings showing bursts of activity were also used to study the voltage dependence of channel current. Fig. 2*D* shows the channel I/V relationship obtained by *averaging* the current amplitudes at each of the different potentials from several different patches ($n = 9$). An estimated mean slope conductance of 75.5 ± 3.0 pS was obtained. Also, it was observed that KcsA showed open channel rectification with mean chord conductances at +200 and −200 mV of 41.8 ± 1.2 pS and 28.4 ± 1.2 pS, respectively. These conductance values are comparable to those reported previously for KcsA reconstituted into planar lipid bilayers (8, 10, 11, 28, 30).

The routine averaging of the current size measurements used for the I/V plots, however, might be misleading, as a closer examination of individual patches reveals that single channel-like openings of clearly different sizes are present in the recordings. Fig. 3 illustrates such variability in recordings taken at +150 mV in which either 4-pA (Fig. 3*A*) or 8-pA (Fig. 3*B*) currents, can be observed as the almost exclusive gating events in each case. The latter 8-pA currents were predominant in most of the patches recorded and in fact, I/V plots obtained from selected recordings showing almost exclusively such currents yielded conductance values very similar to those determined from the "average" measurements from above. Regardless of their frequency of appearance, both the 4- and 8-pA closing and opening events have a single channel-like appearance as far as instrumental resolution distinguishes. This, along with the fact that the larger currents have twice the amplitude of the smaller ones suggests the possibility that, rather than variability in the channel currents, we might be dealing with a phenomenon of coupled gating involving two identical channels acting synchronously. To test this possibility, we proceeded as reported in Kenyon and Bauer (31) by analyzing the amplitude distributions in recordings having 0 (closed states), 4- and 8-pA events to calculate the so-called "coupling parameter," which in all cases yielded values higher than zero, indicating that indeed the openings of the two single channels involved occur cooperatively and are positively coupled. Moreover, we also encountered other recordings in which currents of either 12- or 16-pA currents were detected at +150 mV in the absence of the above 4- or 8-pA currents (not shown) during short but significant periods of time. This suggests that coupling could occasionally go beyond the association of two KcsA channels providing an explanation to the apparently controversial finding of several subconductance states reported earlier (7, 8, 30), in which the possibility of coupled gating as a source of diversity was not considered. Other previously reported channel properties of KcsA, including its selectivity for K^+ or its typical blockade by Na^+ added to the bath solution, mainly at positive voltages, were also found in our experimental system and will not be described here.

Analysis of the HOP Pattern—HOP patterns can be readily distinguished from the LOP patterns from above, because under identical experimental conditions, the channels now remain open most of the time and much more current is conducted through these patches (Fig. 1,

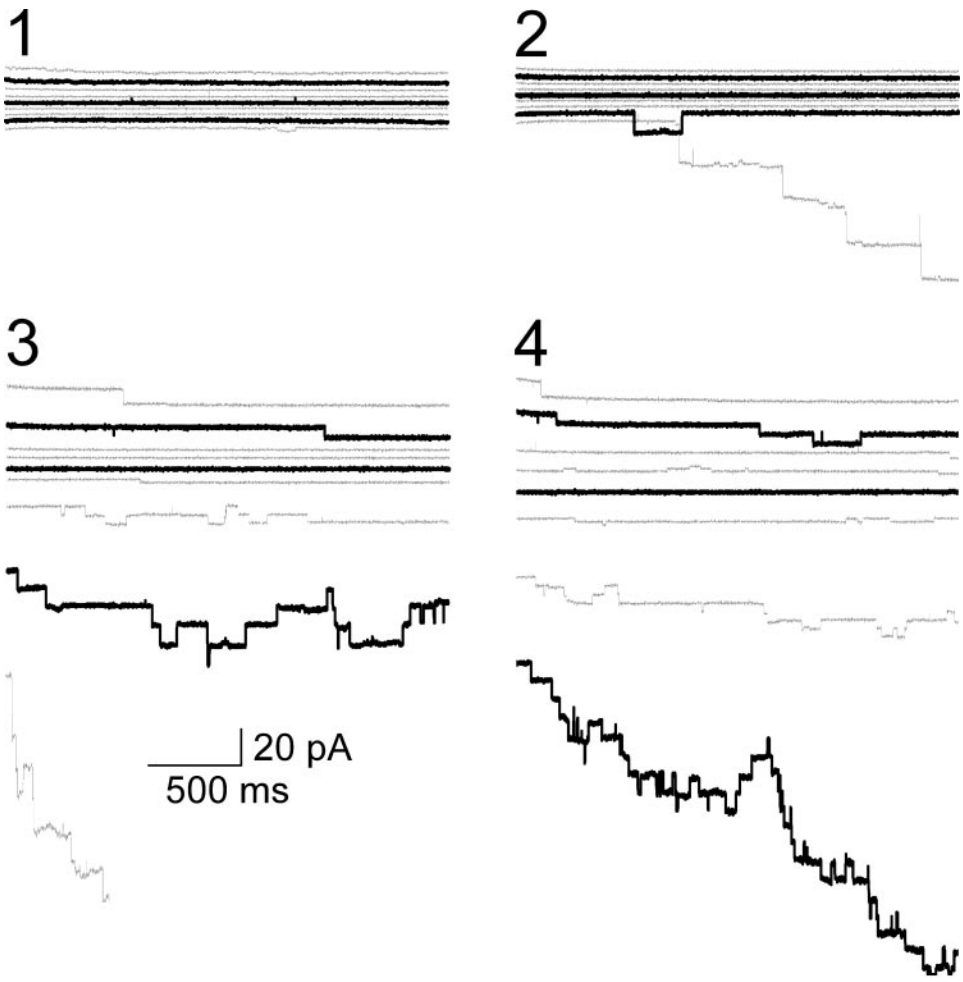

FIGURE 7. **Occasional ladder-like openings exhibited by a small number of patches from KcsA giant liposomes.** The number of open channels increases during the time course of the recording as the protocol of pulses is applied repetitively. Number *1* refers to the first sequence of pulses, while *2*, *3*, and *4* refer to successive pulse sequences applied to the patch at 10- to 20-s intervals. The recordings corresponding to +150, 0, and −150 mV in the successive sequences of pulses have been highlighted in a *thicker trace*.

C and *D*). Fig. 4*A* shows the currents observed at different voltages in the most frequently found HOP pattern, such as that in Fig. 1*C*. Estimates of the open channel probability yielded values as high as 0.9 within the +100 to −100 mV range, with a maximum near 0 mV and decreasing both at extreme negative or positive voltages (Fig. 4*B*). These extreme voltages, which allow for more clear recordings of both channel openings and closings were used to analyze the gating properties of these HOP patterns. Fig. 5*A* shows in detail a representative long recording taken at +150 mV in which three main current levels were observed, each of ~20 pA (equivalent to 133 pS at this voltage), closing successively to finally reach the zero current level. A closer view of the lower 20-pA current level (Fig. 5, *B* and *C*) reveals that, indeed, 20-pA currents were the most frequently observed events and, as far as instrumental resolution permits, appeared mostly as large, single channel-like openings or closings, going all the way from the closed state to the 20-pA current level or *vice versa*. These large 20-pA currents, however, were accompanied by much less frequent, smaller current levels of ~4, 8, 12, and 16 pA, *i.e.* integer multiples of the smaller 4-pA currents. Disregarding the differences in the open channel probability, this is reminiscent of the coupled gating observed in the LOP pattern from above, except that in HOP patterns the coupling seemingly involves up to five 4-pA currents to give rise to the main 20-pA "single" channel events. Unfortunately, the high number of channels involved in this latter putative coupling process prevents the determination of the coupling parameter as done in the LOP patterns from above. The apparent coupling observed in HOP patterns, however, may occasionally be incomplete as shown in Fig. 5*B*, in which the lower 0- to 4-pA current level remains open for some time, as if temporarily excluded from coupling with the other four current levels. Additionally, intense variable flickering, spanning several current levels such as those shown also in Fig. 5*C*, was observed intercalated between regions of coupled gating, as if the ensemble of unitary currents went through periods of variable stability.

In addition to the differences in open channel probability and its voltage dependence, as well as in the degree of the apparent coupled gating, there were other striking differences between HOP and LOP patterns. For instance, channel activity in HOP patterns does not depend on acidic pH anymore and is present at either pH 4 or pH 7 in the bath solution, although the gating features are different (Fig. 6). Also and most remarkably, HOP patterns are not blocked by Na^+, which in fact becomes a conducting species (data not shown). Blockade by Na^+ is considered a hallmark of potassium channels, although in KcsA in particular, a significant Na^+ conduction has been reported previously in the reconstituted planar bilayer system at extreme voltages, in which a "punch-through" mechanism was invoked (32), or in protoplast-liposome vesicle preparations from *Streptomyces* micelia, where a permeability ratio P_K^+/P_{Na}^+ of only three was estimated (7). The above observations on the different pH sensitivity and Na^+ blockade between HOP and LOP patterns strongly indicate that some of the previously reported properties of KcsA may change quite dramatically when in an HOP pattern.

Ladder-like Openings: From No Activity to Building a HOP Pattern—We referred above to a minor population of patches (only 6 out of a total of 93 active patches) in which the main feature is that the number of open channels increases during the time course of the recording as the protocol

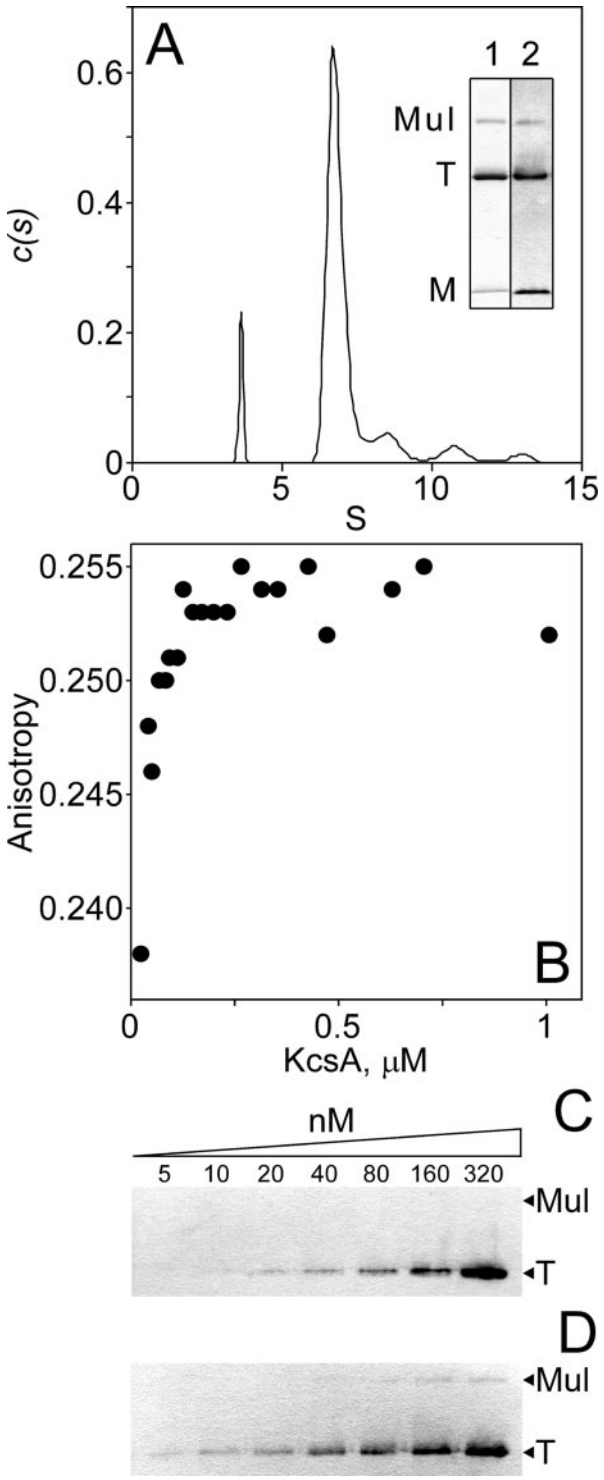

FIGURE 8. **Supramolecular assembly of KcsA in detergent solution.** *A*, apparent sedimentation coefficient distribution derived from sedimentation velocity profiles of detergent-solubilized KcsA (5 μM in terms of KcsA tetramers). Such distribution remained fairly constant within the protein concentration range studied (0.5–10 μM). The *inset* shows typical SDS-PAGE (*lane 1*) and Western anti-His tag immunoblot (*lane 2*) profiles for the purified KcsA preparations used in these studies. *M*, *T*, and *Mul* stand for monomeric, tetrameric, and multimeric KcsA, respectively. *B*, protein concentration dependence of the steady-state fluorescence anisotropy of detergent-solubilized, Alexa 546-labeled KcsA at 25 °C, in a lower protein concentration range (0.025–1 μM). The anisotropy for the free Alexa probe was 0.069. *C*, Western blots from detergent-solubilized KcsA samples to illustrate that tetrameric KcsA remains as the predominant species even under these conditions of low protein concentration, but multimeric KcsA species can hardly be seen. Such multimeric KcsA species in the Western blots, however, can be readily observed at these protein concentrations when reconstituted KcsA samples, instead of detergent-solubilized KcsA, are used in the experiments (*D*).

of pulses is applied repetitively. Fig. 7 shows recordings from one of such patches in which the first group of pulses (numbered '*1*' in Fig. 7) results in essentially no activity at any of the voltages studied. Subsequent recordings (numbered '*2*' to '*4*') taken immediately afterward, however, show that channel openings begin to appear quite conspicuously on top of one another in a ladder-like manner, first at −200 mV, but also at most other voltages in subsequent groups of pulses. Estimation of the size of the current "steps" in the ladder-like ensemble allows distinguishing that, in three out of the six patches showing this behavior, currents corresponding to the unitary current level seen in the LOP or HOP patterns from above, enter or leave the ladder mostly one by one, whereas in the remaining three patches such as that shown in Fig. 7, entering or leaving of pairs of such current levels was observed. Therefore, the same elemental current events seen in the LOP or HOP patterns from above seem also responsible for building up these unusual ladder-like patterns. Eventually, these patches either broke up or become an inward-rectifier type HOP pattern similar to that depicted in Fig. 1*D*, but more importantly, the observation of this ladder-like behavior suggests that the KcsA channels contained in these patches, which are initially inactive, are subjected to a dynamic process that somehow makes them interact with each other in response to the voltage pulses and to acquire a much higher open channel probability.

Evidence for KcsA Clustering—Previous reports on ryanodine (33) or dihydropyridine receptors (34) correlated functional coupling with physical clustering of the channels by evidencing the appearance of a higher sedimentation coefficient species by centrifugation of detergent-solubilized preparations of the channel protein. Here, we carried out analytical ultracentrifugation sedimentation velocity studies in DDM-solubilized KcsA samples at protein concentrations ranging 0.5 to 10 μM. The results show that, regardless of the protein concentration, there is a major sedimenting species of 6.7 S which, depending on the different KcsA preparations, accounted for 80–90% of the total protein (Fig. 8*A*). According to the Svedberg equation (35) and assuming a spherical shape and a 0.73 cm^3/g partial specific volume, the above sedimentation coefficient corresponds to an apparent molecular mass of 110 kDa. This fits fairly well to the theoretical molecular mass of 76 kDa for the KcsA tetramer (160 amino acids per monomer in the native protein, plus 12 additional N-terminal amino acids containing the polyhistidine tag) bound to a reasonable number of DDM molecules. Such putative tetrameric species is accompanied by a lighter species, whose sedimentation coefficient yields an apparent molecular weight similar to that expected from the KcsA monomer, 19 kDa, and by up to three heavier species with average sedimentation coefficients of 9.6, 12.4, and 15.0 S (corresponding to ~190, 280, and 370 kDa, respectively), which altogether accounted for ~10–15% of the total protein in these samples. These observations are somewhat reminiscent of those made using SDS-PAGE (14) in which, in addition to a major band of tetrameric KcsA (the major form in which the purified KcsA runs in SDS-PAGE from non-boiled samples), there is an accompanying band corresponding to KcsA monomer and additional bands heavier than the tetramer, which are more apparent upon reconstitution of the purified KcsA into lipid vesicles and whose molecular weights correspond to the SDS-resistant association into multimers of two or more KcsA tetramers, respectively (see *inset* to Fig. 8*A*).

The possible protein concentration dependence of multimer formation could not be illustrated accurately by analytical centrifugation because of the low 280-nm absorbance in the lower protein concentration range. For this reason, we turned out to use more sensitive fluorescence measurements to study this low protein concentration range. For these experiments, a cysteine-substituted mutant at a strategic site in the KcsA sequence (KcsA S22C) was reacted with sulfhydryl-reactive

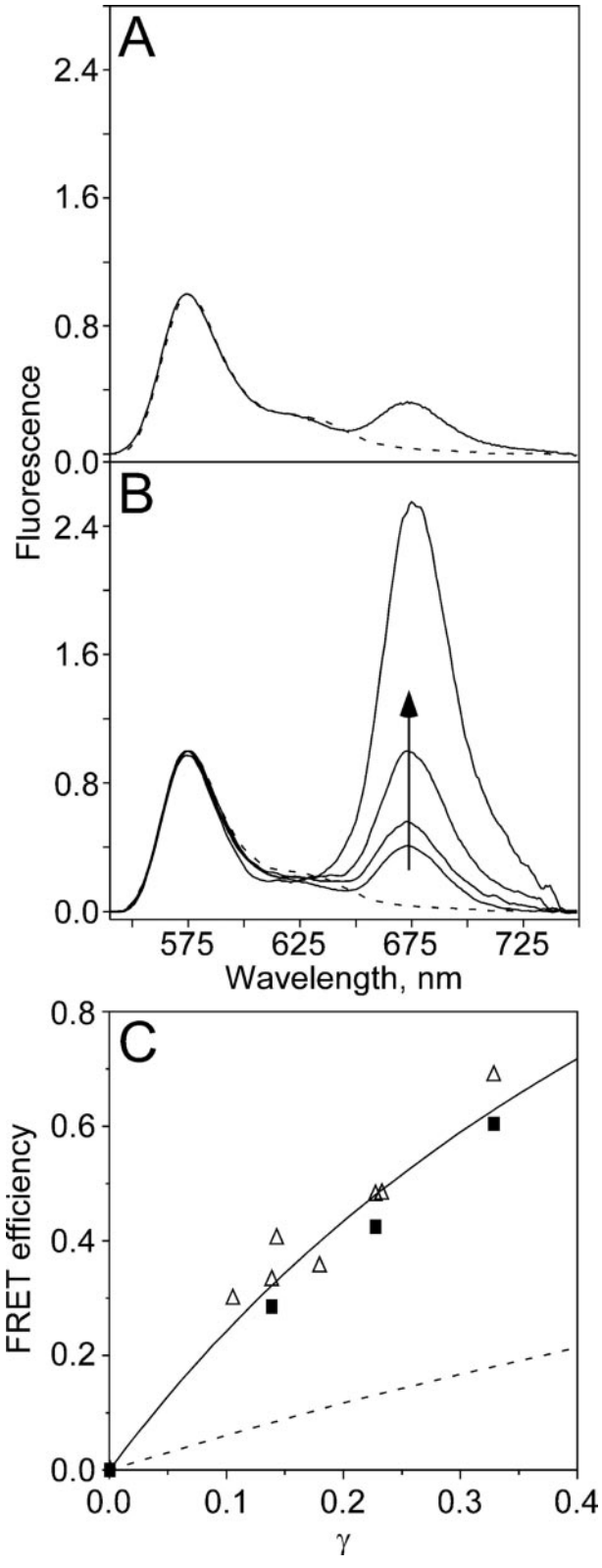

FIGURE 9. **FRET measurements from Alexa 546- and Alexa 647-labeled KcsA as donor and acceptor pair, respectively.** *A*, illustrates the results obtained with detergent-solubilized samples (labeled proteins in 10 mM Hepes, pH 7, 100 mM KCl, 5 mM DDM) at a donor to acceptor ratio of 1:0 and 1:2.1 (*discontinuous* and *continuous lines*, respectively). *B*, results obtained in reconstituted vesicles containing the labeled proteins at varying donor to acceptor ratios (1:0, 1:0.4, 1:0.6, 1:1.7, and 1:10). The *arrow* indicates how the acceptor emission at 675 nm increases as the acceptor is increased with respect to the donor. *C*, estimates of FRET efficiency in reconstituted vesicles determined from either steady-state emission spectra (*opened triangles*) or from donor lifetime measurements (*closed squares*) (see "Experimental Procedures"). The *curve* in the *continuous line* is provided to as a visual guide, whereas the *discontinuous trace* corresponds to the expected theoretical contribution to the FRET signal arising from the random distribution of donor and acceptor molecules in the two-dimensional lipid bilayer. The parameter γ in the *abscissa* measures the acceptor surface density and is equal to the number of acceptor molecules contained within a disk of radius, R_0, the Förster distance (25).

fluorophores (Alexa 546 or 647 maleimide derivatives) to attain fluorescently labeled protein. Fig. 8*B* shows fluorescence anisotropy measurements obtained from the Alexa 546-labeled KcsA. At protein concentrations higher than 0.25 μM, the anisotropy values remain constant and fairly high, as expected from a limited rotational mobility of the relatively large protein species seen in solution. However, at lower concentrations there is a clear concentration dependence of the fluorescence anisotropy, which suggests that the assembly of the larger species from the predominant KcsA tetramers occurs within that concentration range. Such an assembly can be partly reversed by simple dilution of the samples to lower protein concentrations, as shown in Fig. 8. The anisotropy data receive apparent support from simple SDS-PAGE/Western blots (Fig. 8*C*), which indicate that, in detergent-solubilized samples, bands of KcsA multimers can hardly be seen at such low concentrations unless heavily overexposed, whereas they are more easily detected in reconstituted samples containing an identical amount of protein.

The fluorescently labeled Alexa 546 and Alexa 647 KcsA derivatives were also used as donor-acceptor pairs for FRET experiments in detergent solution and in reconstituted vesicles made under identical conditions to those used to prepare the giant liposomes for patch clamp measurements. The R_0 (distance at which there is a 50% efficiency of transfer) was calculated from the spectral overlap as ~68 Å, which seems a sensible distance to monitor supramolecular assembly of KcsA tetramers. Fig. 9 shows that, upon excitation of the donor, there is an increase in acceptor emission as the acceptor:donor ratio is increased, consistent with the occurrence of energy transfer. Such process, however, is less efficient in the detergent-solubilized samples (Fig. 9*A*) than in the reconstituted vesicles (Fig. 9, *B* and *C*), suggesting that reconstitution of the tetrameric KcsA into lipids favors its supramolecular assembly into clusters.

Giant liposomes were also prepared from the reconstituted vesicles containing the fluorescently labeled KcsA in an attempt to visualize the clusters by confocal microscopy. The experimental conditions used in the preparation of such giant liposomes were essentially identical to those used for the recording of KcsA activity by patch clamp techniques. Fig. 10*A* illustrates that the fluorescently labeled protein is distributed heterogeneously in the giant liposomes, defining large (up to micrometer size) highly fluorescent array-like protein complexes on a more homogeneous background containing small fluorescent spots and punctuations of different size throughout. The observed heterogeneity in the distribution of the labeled protein truly responds to the specific association of KcsA molecules, because the distribution of an additional fluorescent phospholipid probe, contained simultaneously in the giant liposomes (Fig. 10*B*), shows that the lipid is distributed much more homogeneously. Thus, the above observations strongly suggest that extensive, heterogeneous clustering of KcsA occurs upon reconstitution into the giant liposomes.

Giant liposomes containing both donor- and acceptor-labeled KcsA at different ratios are also amenable for "*in situ*" FRET measurements by exciting at the appropriate donor excitation wavelength and recording acceptor emission in the confocal microscope (Fig. 11). In agreement with the FRET measurements in the fluorometer cuvette from above, these *in situ* measurements show FRET in the individual giant liposomes between closely arranged donor- and acceptor-labeled KcsA.

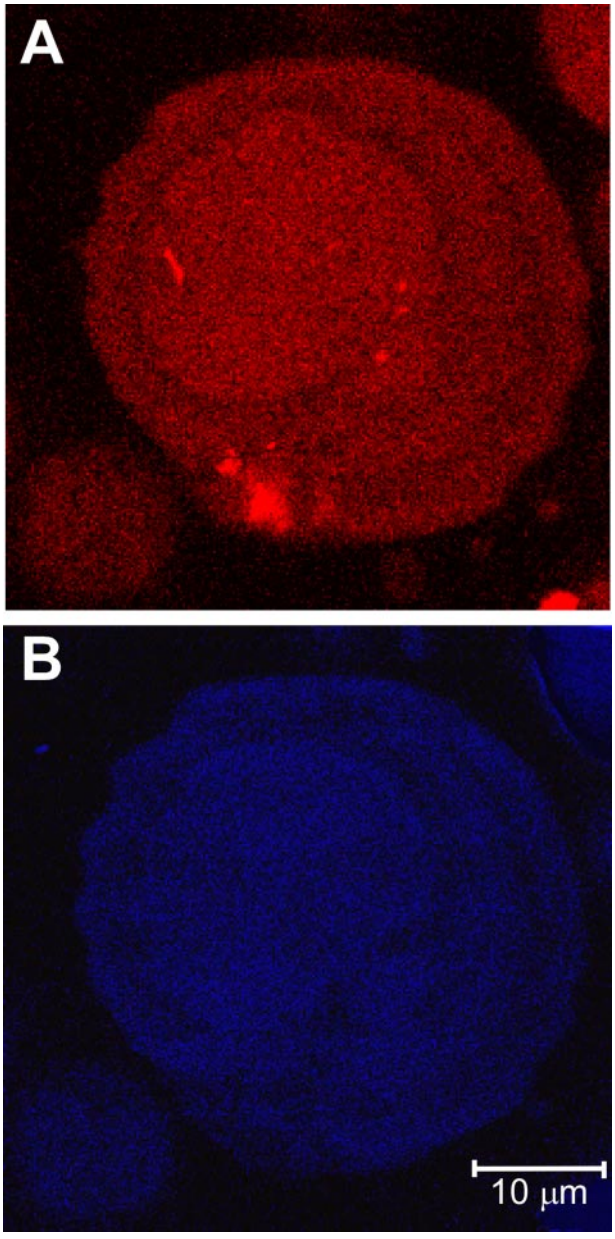

FIGURE 10. *A*, fluorescence microscopy images of KcsA clusters in a confocal cross-section of a giant liposome containing Alexa 546-labeled KcsA. Large and highly fluorescent array-like protein complexes of variable sizes are seen over a more homogeneous protein fluorescence background. In contrast to the marked heterogeneity in the distribution of the KcsA protein from above, *B* shows that the fluorescence of a phospholipid probe (NBD-DMPE) recorded in the same liposome is distributed much more homogeneously.

Moreover, these observations suggests that the larger KcsA clusters are heterogeneous, because they contain regions where energy transfer occurs, along with adjacent regions within the same cluster, which exhibit fluorescence from only the donor- or the acceptor-labeled protein.

DISCUSSION

The more we learn on the different ion channel families, the more we realize that their functional responses are sometimes exquisitely dependent on molecular interactions among themselves or with other cellular components, whose regulatory roles could not be always anticipated from the *in vitro* characterization of the purified channel proteins. Physical clustering of ion channels into closely packed assemblies is among the possible consequences of such intermolecular interactions, and because it is often accompanied by coupled channel gating (33, 36–42) it seems a sensible strategy to secure an optimal ion channel-mediated signaling in response to the appropriate stimuli.

Herein we report that the purified, tetrameric KcsA assembles into clusters of different size. In detergent solution, supramolecular clustering occurs to some extent affecting 10–15% of the total protein. Clustering in detergent solution has been demonstrated by analytical ultracentrifugation, fluorescence anisotropy of the covalently labeled protein, and fluorescence resonance energy transfer using a donor-acceptor pair of KcsA-bound probes. The analytical ultracentrifugation studies show that the KcsA multimers are conformed as discrete sedimenting species with defined stoichiometries, thus excluding the possibility of a nonspecific protein aggregation process. Additionally, the fluorescence anisotropy studies indicate that, even at fairly low protein concentrations, the detergent-solubilized KcsA is subjected to a partly reversible, concentration-dependent equilibrium between cluster-assembled and unassembled forms. Likewise, the efficiency of fluorescence energy transfer between donor- and acceptor-labeled KcsA, which is lower in detergent solution when compared with that seen upon reconstitution of the labeled proteins into lipid vesicles, indicates that the assembly process is clearly favored in the latter conditions. Moreover, confocal microscopy experiments in the reconstituted giant liposomes allow for the visualization of heterogeneous KcsA clusters, some of which reach micrometer size. Additional retrospective evidence to support the clustering of KcsA comes from SDS-PAGE analysis of the purified protein as prepared by most groups working in this field: Bands of molecular weight higher than that corresponding to the characteristic tetramer of four identical subunits (the usual way in which the SDS-resistant KcsA runs in SDS gels) are present both in detergent-solubilized preparations and even more markedly, in reconstituted membranes (14), attesting to the stability (SDS resistance) of some of the building blocks in the clustered forms.

All the above indicates that the tetrameric KcsA has an intrinsic tendency to assemble *in vitro* into heterogeneous supramolecular assemblies or clusters, particularly when reconstituted into membranes. This implies that when a membrane patch is excised from the reconstituted giant liposome for patch clamp recording purposes, there is a finite probability that it would contain KcsA organized in the form of different supramolecular entities, from the more complex large protein arrays to the individual tetrameric protein. According to the observations made in the clustering of receptors (43), clustered assemblies provide the means to convert conformational changes from a single origin into intermolecular allosteric behavior. Indeed, some of the best characterized cases of ion channel clustering, such as ryanodine receptors (33, 37, 38), serotonin 5-hydroxytryptamine2C receptors (40), Kir 4.1 (36), or Kv 2.1 (39) potassium channels, or cystic fibrosis transmembrane conductance regulator chloride channels (41, 42), show that channel activity is dependent on clustering. Therefore, assuming that this would also be the case for KcsA, different channel activity patterns should be expected in the patch clamp recordings arising from the different supramolecular entities present in the giant liposomes. The experimental observation seemingly complies with such an expectation, because different channel activity patterns are in fact detected. The LOP pattern is the most frequently observed and likely represents the simplest mode of assembly of KcsA, because only single channel openings or, more often, gating of two positively coupled channels are detected as the predominant events. The features of the LOP pattern, *i.e.* an acidic pH- and voltage-dependent gating, moderate selectivity for potassium, blockade by sodium, and a very low channel opening probability, essentially coincide with those reported previously for KcsA reconstituted in planar lipid bilay-

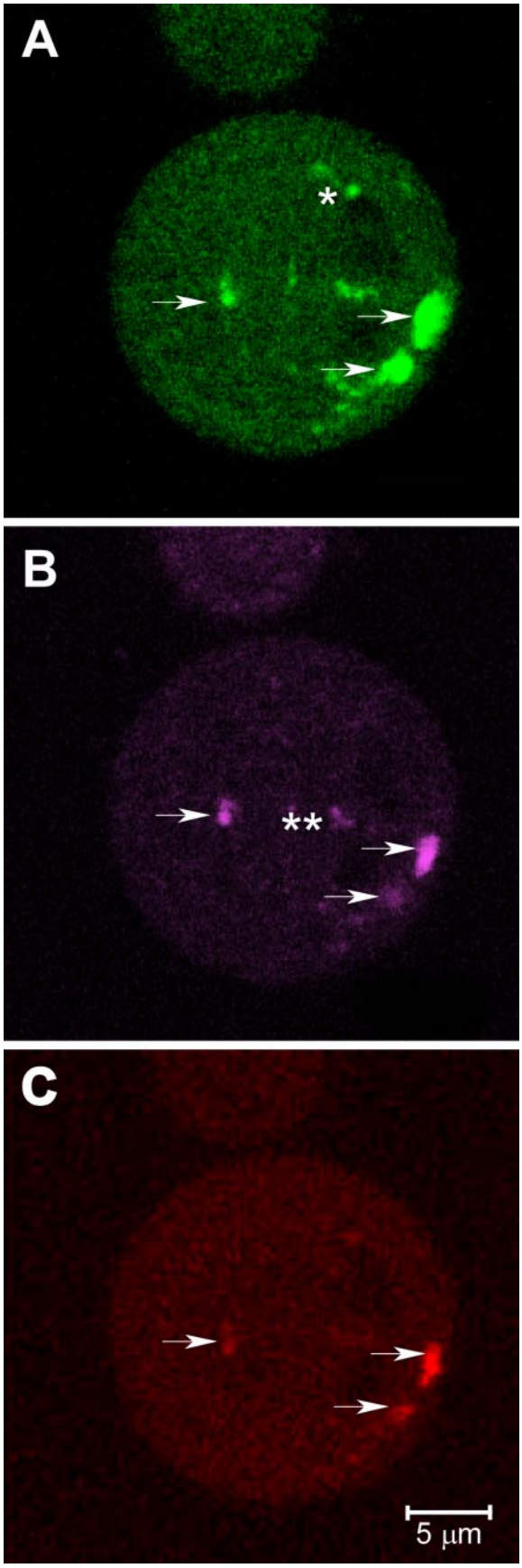

FIGURE 11. **FRET imaging of KcsA clusters.** Giant liposomes containing both Alexa 546- and Alexa 647-labeled KcsA were used in these experiments. Alexa 546 direct emission and FRET fluorescence were recorded simultaneously using the two available channels for simultaneous data acquisition, while direct emission of the Alexa 647-labeled protein was taken immediately afterward. *A–C*, respectively, show images of Alexa 546 (donor) fluorescence, Alexa 647 (acceptor) fluorescence, and the donor to acceptor FRET. The *arrows* indicate the presence of clusters containing both Alexa 546- (*A*) and Alexa 647-labeled KcsA (*B*), in which FRET indeed occurs (*C*). On the contrary, the *single asterisk* in *A* indicates KcsA clusters exhibiting only donor fluorescence; whereas the *double asterisk* in *B* indicates clusters exhibiting only acceptor fluorescence. As expected from the lack of either donor- or acceptor-labeled protein within those clusters (*C*), no FRET occurs at the *single* or *double asterisk regions* in the giant liposomes.

ers (8, 10, 11, 28). Such an apparent equivalence seems consistent with the present findings, because the concentration of protein that became incorporated into planar bilayers is usually very low, and therefore, the protein concentration dependence of the clustering equilibrium as reported here should be displaced to favor the less complex forms of assembly of KcsA. It should be emphasized, however, that the predominant gating event found in our LOP patterns corresponds to the positive coupling of two KcsA channels and that the estimated conductance is practically identical to that reported as the single channel conductance in planar lipid bilayers (see *e.g.* Ref. 11). Thus, it seems likely that similar coupling phenomena might serve to explain previous results (and subsequent discrepancies) on complex, multiple conductance levels reported occasionally for KcsA (7, 8, 28, 30).

HOP patterns have been detected in different forms and, besides their characteristic high channel opening probability, they all have in common frequent events of multiple coupled gating, mostly involving five single channels acting synchronously, and channel opening both at neutral and acidic pH. As to the former, regardless of how many channels might be involved in the concerted multiple openings seen in the HOP patterns, the minimal currents detected seem identical in size to that seen in the LOP pattern, suggesting that the same "building blocks" are used in all possible KcsA assemblies, regardless of their complexity and behavior. Moreover, because the existing reports on channel clustering show that it is often accompanied by coupled gating and increased activity, we interpret our multiple coupled gating and increased channel opening probability in the HOP patterns as a direct consequence of the clustering process. Indeed, the ladder-like HOP patterns (Fig. 7) show how the number of open channels in a given patch increases dramatically during the time course of the recording, likely as a consequence of clustering of the existing channels within the patch. Interestingly, a recent report on clustering of inositol 1,4,5-trisphosphate receptors (44) shows that a conformational change to the *open channel state* is required prior to its assembly into clusters. We do not know whether this would also be the case for KcsA but, certainly, a similar mechanism should be invoked to explain the much increased activity. Indeed, this possibility seems supported by a recent report (45) in which dimers of KcsA tetramers are formed in detergent solution when at pH 5, which favors open channel forms of KcsA, but not at pH 7.

As to the change in pH sensitivity, our observations in the HOP patterns are not completely unprecedented, because the opening of KcsA at neutral pH was found in KcsA when simply subjected to a transmembrane ionic gradient (12). More strikingly, KcsA in the HOP patterns seems to have lost the ability to be blocked by Na^+, which is exhibited only by LOP patterns. Such an apparently controversial finding, however, might be related to existing reports on an altered ionic selectivity and other properties of KcsA reconstituted in different conditions (7, 8, 13) or when subjected to extreme voltages in planar bilayers (32).

The above unexpected changes in the known properties of KcsA when in a HOP pattern might arise from modification or direct involvement of their corresponding molecular determinants in the protein-protein interactions and/or conformational rearrangements involved in the clustering process. For instance, it is known that inward rectification in Kir channels (46) is partly determined by the relative proximity between acidic amino acid res-

idues at strategic sites near the cytoplasmic channel mouth. Such an example provides a nice correlation between a channel feature (inward rectification) and the topology of specific residues, but, because KcsA too has acidic side chains (Glu-118 and Glu-120) near the inner channel mouth whose relative positioning might be affected during clustering, it also provides a plausible hypothesis to explain the inward rectification observed in some of the HOP patterns reported here.

Concentration-dependent clustering in protein solutions and colloids has been attributed to a combination of short range attractive and long range electrostatic repulsive forces (47). In KcsA, both the C- and N-terminal regions in the protein sequence are rich in charged amino acid side chains, and therefore, they appear as potential candidates to act as molecular determinants for cluster formation and integrated behavior. In this respect, preliminary experiments using 1–125 KcsA obtained from chymotrypsin cleavage of full-length 1–160 KcsA show clustering and HOP patterns undistinguishable from those of the wild-type protein, *i.e.* indicating that the large 126- to 160-amino acid C-terminal portion of the protein is not involved in these processes (not shown). The possible roles of the N-terminal or the transmembrane segments of the protein in these processes are presently still under investigation, and additional work is needed to reach more definitive conclusions on this issue.

The finding that KcsA, one of the structurally simplest ion channels known to date, shows such a complex clustering and coupled gating behavior "*in vitro*" is surprising. We do not know enough about the biology of *Streptomyces* to be able to say whether these phenomena would also happen "*in vivo*" and serve any physiological purpose. However, the molecular crowding expected *in vivo*, along with the protein concentration dependence observed in the *in vitro* process, makes it likely that clustering would also occur in the bacterial membrane. Nevertheless, it should be noted that our *in vitro* observations probably correspond to deregulated clustering processes, because the putative anchoring molecules needed *in vivo*, if any, would not be present in our purified, recombinant KcsA preparations. In KcsA in particular, polyphosphates and polyhydroxybutyrate, which are abundant reservoir materials in prokaryotic cells, have been reported to interact with KcsA to form conductive complexes (13, 48). Therefore, these or similar compounds, such as prokaryotic alternatives to PDZ-domains or other anchoring proteins observed in the clustering of other channels (33, 41, 42, 49), might provide a clue as to where to start looking for potential cluster-inducing or cluster-stabilizing molecules. Thus far, however, it seems reasonable to assume that KcsA clustering, coupled gating, and channel opening at neutral pH with high probability, may be more biologically meaningful than the currently established view of KcsA opening only at very acidic intracellular pH and with very low probability.

Acknowledgments—We are indebted to our colleagues Dr. Roberto Gallego (Instituto de Neurociencias, Universidad Miguel Hernández) and Dr. Andrés Morales (Departamento de Fisiología, Universidad de Alicante) for critical reading of the manuscript. We also thank Dr. F. Sala and Dr. S. Sala (Instituto de Neurociencias, Universidad Miguel Hernández) and Dr. Germán Rivas and Dr. Carlos Alfonso (Centro de Investigaciones Biológicas, Consejo Superior de Investigaciones Científicas, Madrid) for their help with the patch clamp and the analytical ultracentrifugation experiments, respectively. Eva Martínez provided excellent technical help throughout.

REFERENCES

1. Booth, I. R., Edwards, M. D., and Miller, S. (2003) *Biochemistry* **42,** 10045–10053
2. MacKinnon, R. (2003) *FEBS Lett.* **555,** 62–65
3. Doyle, D. A. (2004) *Mol. Membr. Biol.* **21,** 221–225
4. Armstrong, C. M. (2003) *Sci. STKE 2003,* RE10
5. Doyle, D. A., Morais, C. J., Pfuetzner, R. A., Kuo, A., Gulbis, J. M., Cohen, S. L., Chait, B. T., and MacKinnon, R. (1998) *Science* **280,** 69–77
6. Zhou, Y., Morais-Cabral, J. H., Kaufman, A., and MacKinnon, R. (2001) *Nature* **414,** 43–48
7. Schrempf, H., Schmidt, O., Kummerlen, R., Hinnah, S., Muller, D., Betzler, M., Steinkamp, T., and Wagner, R. (1995) *EMBO J.* **14,** 5170–5178
8. Meuser, D., Splitt, H., Wagner, R., and Schrempf, H. (1999) *FEBS Lett.* **462,** 447–452
9. Splitt, H., Meuser, D., Borovok, I., Betzler, M., and Schrempf, H. (2000) *FEBS Lett.* **472,** 83–87
10. Heginbotham, L., LeMasurier, M., Kolmakova-Partensky, L., and Miller, C. (1999) *J. Gen. Physiol.* **114,** 551–560
11. LeMasurier, M., Heginbotham, L., and Miller, C. (2001) *J. Gen. Physiol.* **118,** 303–314
12. Zakharian, E., and Reusch, R. N. (2004) *Biochem. Biophys. Res. Commun.* **316,** 429–436
13. Zakharian, E., and Reusch, R. N. (2004) *Biochem. Biophys. Res. Commun.* **322,** 1059–1065
14. Molina, M. L., Encinar, J. A., Barrera, F. N., Fernandez-Ballester, G., Riquelme, G., and Gonzalez-Ros, J. M. (2004) *Biochemistry* **43,** 14924–14931
15. Riquelme, G., Lopez, E., Garcia-Segura, L. M., Ferragut, J. A., and Gonzalez-Ros, J. M. (1990) *Biochemistry* **29,** 11215–11222
16. Hamill, O. P., Marty, A., Neher, E., Sakmann, B., and Sigworth, F. J. (1981) *Pflugers Arch.* **391,** 85–100
17. Laemmli, U. K. (1970) *Nature* **227,** 680–685
18. Schuck, P. (2000) *Biophys. J.* **78,** 1606–1619
19. Gonzalez, J. M., Velez, M., Jimenez, M., Alfonso, C., Schuck, P., Mingorance, J., Vicente, M., Minton, A. P., and Rivas, G. (2005) *Proc. Natl. Acad. Sci. U. S. A.* **102,** 1895–1900
20. Lackowicz, J. R. (1999) *Principles of Fluorescence Spectroscopy*, pp. 291–391, Plenum Press, New York
21. Selvin, P. R. (2002) *Annu. Rev. Biophys. Biomol. Struct.* **31,** 275–302
22. Panchuk-Voloshina, N., Haugland, R. P., Bishop-Stewart, J., Bhalgat, M. K., Millard, P. J., Mao, F., Leung, W. Y., and Haugland, R. P. (1999) *J. Histochem. Cytochem.* **47,** 1179–1188
23. James, D. R., Siemiarczuk, A., and Ware, W. R. (1992) *Rev. Sci. Instrum.* **63,** 1710–1716
24. Liu, R., Siemiarczuk, A., and Sharom, F. J. (2000) *Biochemistry* **39,** 14927–14938
25. Capeta, R. C., Poveda, J. A., and Loura, L. M. (2006) *J. Fluoresc.* **16,** 161–172
26. Wolber, P. K., and Hudson, B. S. (1979) *Biophys. J.* **28,** 197–210
27. Choi, H., and Heginbotham, L. (2004) *Biophys. J.* **86,** 2137–2144
28. Cuello, L. G., Romero, J. G., Cortes, D. M., and Perozo, E. (1998) *Biochemistry* **37,** 3229–3236
29. Irizarry, S. N., Kutluay, E., Drews, G., Hart, S. J., and Heginbotham, L. (2002) *Biochemistry* **41,** 13653–13662
30. Meuser, D., Splitt, H., Wagner, R., and Schrempf, H. (2001) *Eur. Biophys. J.* **30,** 385–391
31. Kenyon, J. L., and Bauer, R. J. (2000) *J. Neurosci. Methods* **96,** 105–111
32. Nimigean, C. M., and Miller, C. (2002) *J. Gen. Physiol.* **120,** 323–335
33. Marx, S. O., Gaburjakova, J., Gaburjakova, M., Henrikson, C., Ondrias, K., and Marks, A. R. (2001) *Circ. Res.* **88,** 1151–1158
34. Wolf, M., Eberhart, A., Glossmann, H., Striessnig, J., and Grigorieff, N. (2003) *J. Mol. Biol.* **332,** 171–182
35. Cole, J. M., and Hansen, J. C. (1999) *J. Biomol. Tech.* **10,** 163–176
36. Horio, Y., Hibino, H., Inanobe, A., Yamada, M., Ishii, M., Tada, Y., Satoh, E., Hata, Y., Takai, Y., and Kurachi, Y. (1997) *J. Biol. Chem.* **272,** 12885–12888
37. Laver, D. R., O'Neill, E. R., and Lamb, G. D. (2004) *J. Gen. Physiol.* **124,** 741–758
38. Yin, C. C., Blayney, L. M., and Lai, F. A. (2005) *J. Mol. Biol.* **349,** 538–546
39. Misonou, H., Mohapatra, D. P., Park, E. W., Leung, V., Zhen, D., Misonou, K., Anderson, A. E., and Trimmer, J. S. (2004) *Nat. Neurosci.* **7,** 711–718
40. Herrick-Davis, K., Grinde, E., Harrigan, T. J., and Mazurkiewicz, J. E. (2005) *J. Biol. Chem.* **280,** 40144–40151
41. Raghuram, V., Mak, D. D., and Foskett, J. K. (2001) *Proc. Natl. Acad. Sci. U. S. A.* **98,** 1300–1305
42. Wang, S., Yue, H., Derin, R. B., Guggino, W. B., and Li, M. (2000) *Cell* **103,** 169–179
43. Bray, D., and Duke, T. (2004) *Annu. Rev. Biophys. Biomol. Struct.* **33,** 53–73
44. Tateishi, Y., Hattori, M., Nakayama, T., Iwai, M., Bannai, H., Nakamura, T., Michikawa, T., Inoue, T., and Mikoshiba, K. (2005) *J. Biol. Chem.* **280,** 6816–6822
45. Zimmer, J., Doyle, D. A., and Grossmann, J. G. (2005) *Biophys. J.* **90,** 1752–1766
46. Pegan, S., Arrabit, C., Zhou, W., Kwiatkowski, W., Collins, A., Slesinger, P. A., and Choe, S. (2005) *Nat. Neurosci.* **8,** 279–287
47. Stradner, A., Sedgwick, H., Cardinaux, F., Poon, W. C., Egelhaaf, S. U., and Schurtenberger, P. (2004) *Nature* **432,** 492–495
48. Reusch, R. N. (1999) *Biochemistry* **38,** 15666–15672
49. Marx, S. O., Ondrias, K., and Marks, A. R. (1998) *Science* **281,** 818–821